Characterization and quantification methods of complex BCC matrix microstructures in advanced high strength steels

Kangying Zhu · David Barbier · Thierry Iung

Abstract The development of comprehensive and reliable microstructure characterization tools is very necessary for the understanding and modelling of both the formation of different phases during processing and the relationship between microstructure and mechanical properties. A series of samples containing different phases with a BCC structure have been characterised using different techniques including optical microscopy (OM), field emission gun scanning electron microscopy (FEG-SEM) with secondary electron (SE) and back scattered electron (BSE) modes, electron back scattered diffraction (EBSD) and transmission electron microscopy (TEM). It is shown that it is difficult to distinguish ferrite from bainite especially granular bainitic ferrite using conventional OM and FEG-SEM (SE) techniques, whereas FEG-SEM (BSE) and EBSD are the most suitable techniques to differentiate them. A new EBSD method has been developed to dissociate and quantify ferrite, bainite and martensite in multi-phase AHSS steels. This method has been proven to be pertinent and has been validated using reference specimens.

Introduction

Most of the advanced high strength steels (AHSS) display complex multi-phase microstructures. During continuous cooling and/or isothermal holding after deformation of hot rolled products or after intercritical annealing of cold rolled products, there is often a successive formation of ferrite, different kinds of bainite, as well as fresh or tempered martensite. The precise characterization of the complex microstructure of these multi-phase steels is of great importance for the understanding and modeling of both the formation of different phases during processing and the relationship between microstructure and properties. Presently, the distinction and quantification of these phases are still a big issue. The development of reliable and powerful microstructure characterization tools is very necessary for the optimisation of mechanical properties of these materials.

Different characterization methods for the complex microstructure of these steels are available. Optical microscopy (OM) observations after coloured etching coupled with image analysis are commonly used to characterise complex microstructures of low-alloyed steels. For example, LePera etching allows the distinction of ferrite and bainite from austenite and martensite; some tint etchant that contains sodium metabisulfite ($Na_2S_2O_5$) can differentiate bainite and martensite from ferrite [1, 2]. But this conventional metallographic method displays two drawbacks: (1) OM reaches its limitation in resolution to reveal the very fine microstructures of the modern AHSS steels; (2) the phase distinction is based on colour difference under OM, but the phase etching colour mainly depends on the local carbon content [3], which may lead to a colour gradient for a given phase. For instance, after Lepera etching, the carbon-rich phases like austenite and fresh martensite both appear white, whereas bainite may appear brownish to white depending on its residual carbon content and dislocation density. In addition, the etching colour of different phases varies very much as a function of the etchant, etching temperature and time, air humidity, as well as sample surface condition.

K. Zhu (✉) · D. Barbier · T. Iung
ArcelorMittal Maizières, Research and Development, Voie Romaine, BP30320, 57283 Maizières-lès-Metz Cedex, France
e-mail: kangying.zhu@arcelormittal.com

D. Barbier
e-mail: david.barbier@arcelormittal.com

T. Iung
e-mail: thierry.iung@arcelormittal.com

X-ray or neutron diffraction can be used to measure the volume fraction of austenite but is incapable of dissociating ferrite, bainite and martensite. During recent years, SEM together with EBSD technique has been more and more applied to distinguish different phases and to determine their volume fractions. Retained austenite and ferrite can be easily separated using EBSD since they have different crystallographic structure. In addition, the Kikuchi pattern quality is sensitive to lattice defects. Martensite has a low pattern quality or image quality (IQ) and it cannot even be indexed when its carbon content is very high. Wilson et al. [4] separated martensite from ferrite in a DP steel simply using a threshold IQ value of the pixels. The obtained martensite fraction is in good agreement with the result stemming from the point counting method when the IQ profile exhibits a clear bimodal distribution. But this simple method becomes unreliable when there is considerable peak overlap. Wu et al. [5] dissociated the IQ profile of all the pixels using several Gaussian peaks, and then the volume fraction of each phase could be estimated from the peak area. However, this method is unable to keep the link between the IQ profile data and the microstructure map data, therefore the information on the locations and orientations of the pixels that contribute to each Gaussian peak is lost and further analyses on grain size and texture for each phase are impossible. By contrast, the method that differentiates the phases with grain unit using grain average functions (like mean band contrast) as criteria to keep a metallurgical sense seems more promising [6]. It is to be clarified that IQ and band contrast (BC) are equivalent terms to describe the quality of the Kikuchi pattern, except that IQ is the output of TSL OIM software, whereas BC is the output of Channel 5 HKL software for EBSD analysis.

The dissociation of bainitic ferrite from ferrite is proven to be difficult and needs more efforts, as these two phases are crystallographically identical. In the literature, IQ, confidence index (CI) and band slope (BS) have been employed to distinguish bainite from ferrite since bainite contains a larger amount of lattice defects than ferrite, leading to a lower IQ, CI and BS [7–10]. Nevertheless, no clear quantitative criteria have been established to discriminate the pixels that belong to ferrite or bainite. More recently, Zaefferer et al. tested a method which was based on the calculation of Kernel average misorientation (KAM) maps to detect the small orientation gradients created by the bainitic transformation in an Al-containing TRIP steel. The threshold for the KAM value that differentiates ferrite and bainitic ferrite was determined with the aid of a software tool based on the analysis of the boundaries between these two phases [11]. This procedure seems to give a satisfactory separation between the two BCC components.

In this study, different techniques including OM, SEM with secondary electron (SE) mode and back scattered electron (BSE) mode, EBSD and TEM have been compared to identify and distinguish different phases: ferrite, various types of bainite and martensite. As compared with previous published work, the phase separation and quantification method using EBSD data proposed in this paper are based on grain unit mode instead of pixel mode, which avoids the problem that pixels belonging to the same grain are frequently considered as different phases. Clear and new quantitative criteria including mean grain BS, grain internal mean misorientation (GIMM), grain size and shape have been defined to dissociate different ferritic phases, especially ferrite from bainite.

Experimental methods

A series of specimens containing various microstructures (ferrite, bainite in the granular or lath form and martensite) have been selected for the study. Their corresponding chemical compositions and process or heat treatment conditions are listed in Table 1. The thermal treatments of samples A–E were carried out using a Bähr DIL805 dilatometer. Sample A and E were cut from 1.2-mm thick cold rolled sheets and have a dimension 4 × 10 × 1.2 (mm), whereas samples B, C and D are cylindrical (Φ4 × 10 mm) specimens being cut from a 7-mm thick hot rolled sheet. The microstructures of samples A–E will be described in detail in "Description of the microstructures in the different samples" section. Sample F was subjected to a hot rolling process followed by a controlled cooling pattern which gives a mixed ferrite and martensite microstructure.

Microstructural characterizations were carried out by means of different techniques: OM, field emission gun scanning electron microscopy (FEG-SEM) with SE or BSE mode, electron back scattered diffraction (EBSD) and transmission electron microscopy (TEM). FEG-SEM examinations were performed on a Jeol JSM-7001F microscope equipped with an EBSD fast acquisition system. Channel 5 HKL software is used to process EBSD data. Thin foils for transmission electron microscopy were prepared using the twin-jet method and observed in a Philips CM200 FEG microscope.

Identification of phases

Definition of phases

In order to distinguish the different phases, the first thing to be clarified is the definition of ferrite and different types of bainite, especially granular bainite which is a subject of controversy in the literature. For instance, some researchers considered that the granular bainite consists of equiaxed bainitic ferrite matrix containing secondary phase islands and the temperature range to form granular bainite is

Table 1 Chemical compositions and heat treatment conditions of studied samples

Sample	Chemical composition (wt%)				Heat treatment condition
	C	Mn	Si	Cr	
A	0.015	1.54			Austenitization at 1000 °C for 10 min, followed by a cooling to room temperature at a constant cooling rate of 4.4 °C/s
B	0.051	1.49	0.3		Austenitization at 1250 °C for 10 min, followed by a rapid quench to 600 °C, and then a holding at 600 °C for 15 min with a final quench to room temperature
C	0.051	1.49	0.3		Austenitization at 1250 °C for 10 min, followed by a rapid quench to 550 °C, and then a holding at 550 °C for 15 min with a final quench to room temperature
D	0.15	1.9	0.2	0.2	Austenitization at 820 °C for 60 s, followed by a cooling at 18 °C/s to 460 °C, and then a holding at 460 °C for 30 s with a final quench to room temperature
E	0.15	1.9	0.2	0.2	Intercritical annealing at 780 °C for 10 min, followed by a rapid quench to 460 °C, and then a holding at 460 °C for 10 min with a final quench to room temperature
F	0.07	0.93	0.2	0.7	Hot rolled sample: finish rolling at 780 °C, followed by an air cooling to 730 °C, then a rapid quench to 200 °C and coiling at 200 °C

slightly higher than that of the upper bainite [12, 13]. Other researchers regarded granular bainite as fairly recovered bainite with a "lath-less" morphology [14]. The Bainite Research Committee of The Iron and Steel Institute of Japan has proposed a specific terminology to describe the five possible ferrite morphologies [15]. Among them, (i) quasi-polygonal ferrite (QF) is characterised by grains with undulating boundaries which may cross prior austenite boundaries and containing a dislocation substructure and/or occasional martensite/austenite (M/A) micro-constituents, (ii) granular ferrite (GF) consists of sheaves of elongated ferrite with low misorientations and a high dislocation density, sometimes containing roughly equiaxed islands of M/A micro-constituents. It is frequently very difficult to distinguish QF grains from often-ragged GF sheaves using OM and even TEM, for the reason that both QF and GF contain dislocation substructure features [16]. In our study, both QF and GF are considered as granular bainite.

Apart from granular bainite, ferrite is the equilibrium microstructural constituent containing a very low dislocation density and no substructure. Lath bainite structure consists of packets of parallel ferrite laths (or plates) and can be divided into upper bainite and lower bainite according the grain boundary misorientation distribution: upper bainite displays fewer high angle boundaries (misorientations > 50°) but a greater number of low angle boundaries, whereas lower bainite exhibits a high proportion of boundaries with misorientations in the range 50°–60° and very few boundaries with low misorientations (<20°) [17]. Lath bainite structure was often defined as upper or lower bainite according to carbide distribution (inter-lath or intra-lath) in the literature [18–21]. In our work, grain boundary misorientation distribution criterion is selected since it can be adapted to all kinds of lath bainite structure including carbide-free bainitic lath structure.

The distinction and quantification of ferrite from granular bainite is important since granular bainite is known to contribute to an increased strength, low yield-to-ultimate-strength ratios and high strain-hardening rates, through increased dislocation density and sometimes M/A constituents, while maintaining a reasonable level of toughness [22, 23].

Description of the microstructures in the different samples

The resulting microstructures after heat treatment for each sample are given in Table 2. Among them, samples A, B and C were selected to test the different characterisation techniques with the aim to find out the best method to identify ferrite, granular bainite and lath bainite. Sample C was further used to confirm the reliability of FEG-SEM with BSE mode to characterise the substructure. Samples D, E and F having different combinations of ferrite, bainite and martensite fractions were employed to test and to validate the new phase quantification method.

Table 2 Microstructures of the studied samples

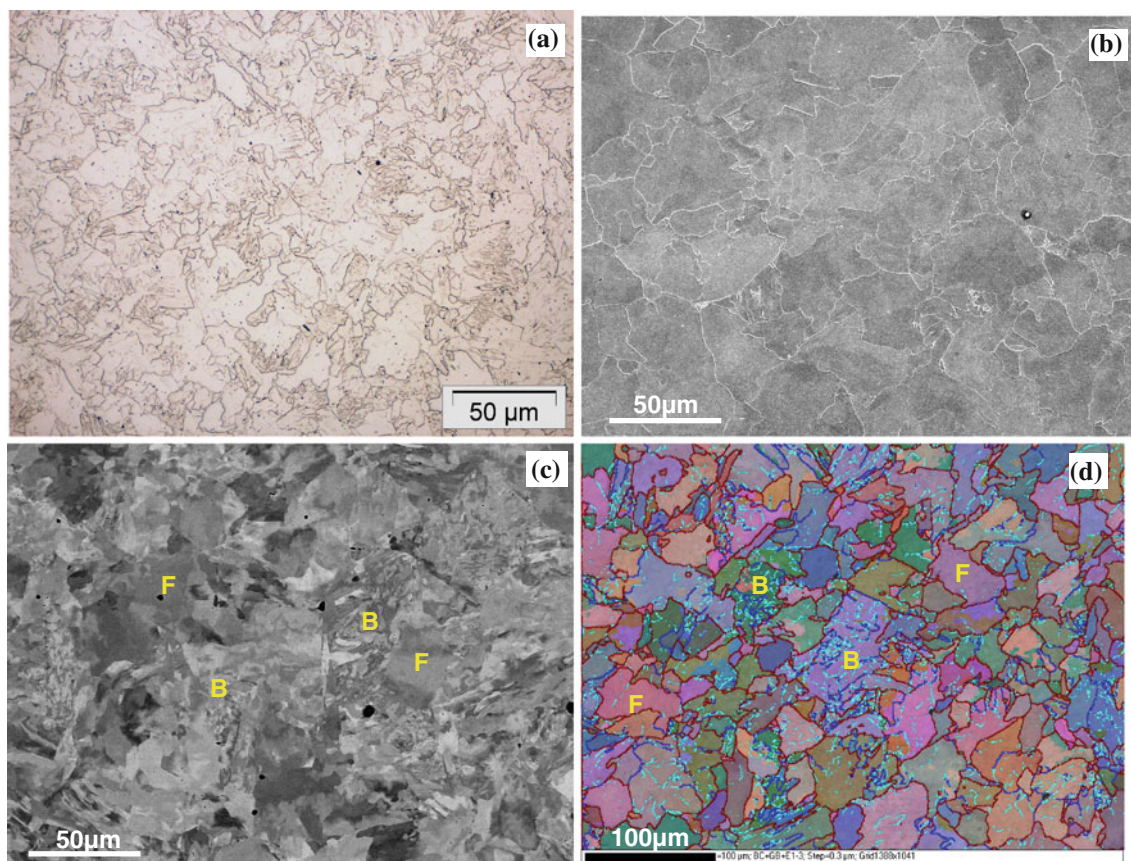| Sample	Microstructure
A	Equiaxed ferrite + granular bainite (without secondary phase)
B	Allotriomorphic ferrite + granular bainite + lath bainite
C	Very few granular bainite + lath bainite
D	Equiaxed ferrite + bainite (granular and lath) + martensite (fresh and tempered)
E	Equiaxed ferrite + bainite (granular and lath)
F	Equiaxed ferrite + martensite + few bainite grains

Fig. 1 Microstructural observations of sample A using (**a**) OM after Nital etching, (**b**) FEG-SEM with SE mode, (**c**) FEG-SEM with BSE mode, and (**d**) EBSD orientation map using the all-Euler angles colouring scheme for sample A: grain boundaries with misorientations 2°–5° in *light blue colour*, misorientations 5°–20° in *blue colour*, and misorientations above 20° in *dark red colour*. *F* ferrite, *B* bainite (Color figure online)

Identification of ferrite and bainite

This study has been performed on samples A, B and C. Their microstructures have been characterised using OM, FEG-SEM-EBSD and TEM. Figure 1 compares the microstructure of sample A observed by means of different techniques. It should be noted that the start and finish phase transformation temperatures of this sample are estimated to be around 710 and 600 °C, respectively, from the dilatometry signal. Moreover, the Bs temperature is calculated to be 690 °C according to the Steven formula [24]. Therefore, it is reasonable to consider that the microstructure of sample A contains both ferrite and bainite. Very irregular grain boundaries can be observed for this sample using OM (Fig. 1a), which gives the impression that the microstructure contains mainly granular bainitic ferrite and it is very difficult to recognize any equiaxed ferrite in the microstructure. No more information can be obtained using FEG-SEM with SE mode (Fig. 1b). It is possible to obtain evidence for certain substructures in the granular bainitic ferrite by SEM after a very heavy etching [25]. But heavy etching may also lead to a loss of information on small constituents like

cementite or MA islands. A good crystallographic contrast obtained using FEG-SEM with BSE mode allows to distinguish ferrite from granular bainitic ferrite: ferrite exhibits a uniform contrast inside the grains, whereas the granular bainite displays a varied contrast due to the substructures inside (Fig. 1c). The colour of the all-Euler EBSD image in Fig. 1d indicates the orientation of grains. Some grains which are observed to display a uniform colour and no subgrain boundaries inside (misorientation < 15°) should correspond to ferrite, whereas others which have a variation in colour and with subgrain boundaries inside should correspond to bainitic ferrite. Therefore, there is a good qualitative consistence between the microstructure obtained by FEG-SEM with BSE mode and EBSD technique.

Figure 2 gives another example of the microstructure characterisation using OM and FEG-SEM with BSE mode. It can be observed under OM (Fig. 2a) that sample B has a rather complex microstructure: some areas exhibit a granular morphology with irregular grain boundaries whereas other areas display a lath-like morphology, and it exists also a small quantity of secondary phase islands in dark colour which were confirmed to be pearlite and martensite
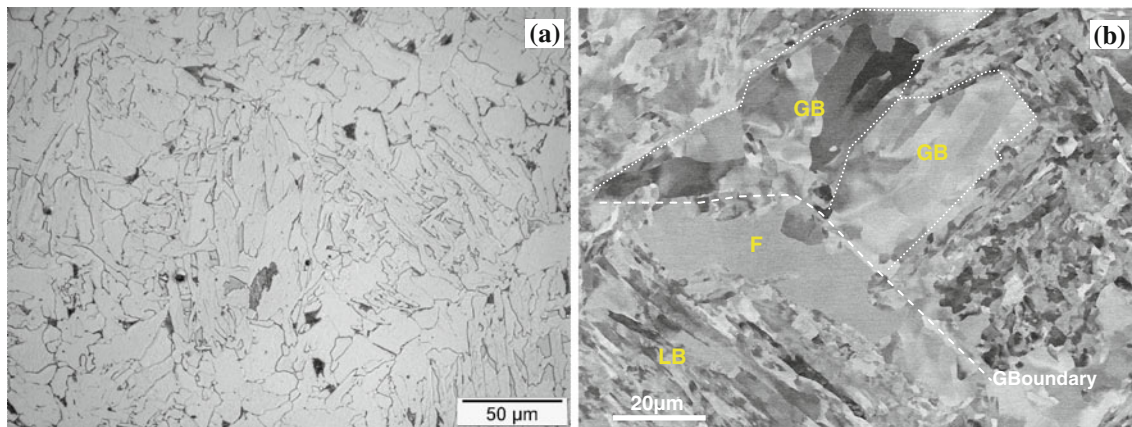
Fig. 2 Microstructural observations of sample B using (**a**) OM after Nital etching and (**b**) FEG-SEM with BSE mode. *F* ferrite, *GB* granular bainite, *LB* lath bainite. GBoundary-prior austenite grain boundary

islands with FEG-SEM (SE mode). The microstructure details of this sample are revealed by FEG-SEM with BSE mode (Fig. 2b): (1) a few allotriomorphic ferrite grains, which may form during rapid cooling or at the beginning of the holding at 600 °C, locate at the prior austenite grain boundaries; (2) granular bainitic grains contain either granular substructures or large laths with a width in the range 2–7 μm. The misorientation of these subgrain boundaries of large lath boundaries is so small that they are difficult to be etched and thus difficult to be detected using OM or FEG-SEM with SE mode; (3) lath bainitic structure is composed of packets of fine laths with a width in the range 0.2–1 μm. Some of these lath boundaries have a high enough misorientation to be etched easily and then to be observed under OM. The areas with a lath-like morphology under OM correspond to lath bainite structure.

It should be mentioned that in many papers in the literature, granular bainite is often distinguished from ferrite using conventional OM and/or SEM (SE mode) techniques without the help of BSE mode, EBSD or TEM [26–30]. However, it is shown from our investigations that ferrite is indeed very difficult to be differentiated from granular bainite using only OM and/or SEM with SE mode.

The microstructures of samples B and C have also been characterised using EBSD technique. The EBSD images and the corresponding grain boundaries misorientation distribution profiles of these two samples are shown in Fig. 3. The boundaries with a misorientation between 20° and 48° are in red and those with a misorientation higher than 48° are in black. It can be seen in Fig. 3a that, the grains in sample B exhibit three morphologies, as indicated by 1, 2, 3 in the figure: some granular grains with a uniform colour indicating no variation in orientation inside correspond to equiaxed ferrite; other granular grains with a variation in colour suggesting the presence of substructure inside correspond to granular bainite; and the remaining grains containing large packets of lowly misoriented laths (<20°) correspond to lath

bainite structure. This observation is in very good agreement with the microstructure in Fig. 2b, characterised using FEG-SEM with BSE mode. It is worth mentioning that almost all the granular grains (equiaxed ferrite or granular bainite) are surrounded by grain boundaries with a misorientation between 20° and 48°. When the holding temperature is decreased from 600 °C (sample B) to 550 °C (sample C), the microstructure (Fig. 3b) becomes more and more in a lath form and very few granular grains can be found. In this case, the frequency of the grain boundaries with a misorientation between 20° and 48° becomes almost nil (Fig. 3d). It can be identified from the grain boundary misorientation distribution profiles in Fig. 3c, d that the lath bainite structure in samples B and C is upper bainite.

Sample C has been analysed using both TEM and FEG-SEM (BSE) (Fig. 4) to evaluate the possibility of using FEM-SEM (BSE) to replace TEM. It can be seen from Fig. 4 that even the dislocation configurations in the material cannot be investigated using FEG-SEM (BSE) and the resolution of the TEM image is much better, FEG-SEM (BSE) is sensitive to very weakly misoriented subgrain boundaries. A similar lath size of bainite can be obtained using these two techniques.

Quantification of phases

It is shown from the aforementioned analysis that FEG-SEM (BSE) and EBSD techniques are the most adapted methods to distinguish ferrite from bainite. So, there is a potential to develop an automatic phase quantification method using EBSD data.

Possible parameters to differentiate phases with EBSD data

Since the quality of Kikuchi pattern is closely connected with the defects in the lattice, both BC, which describes the
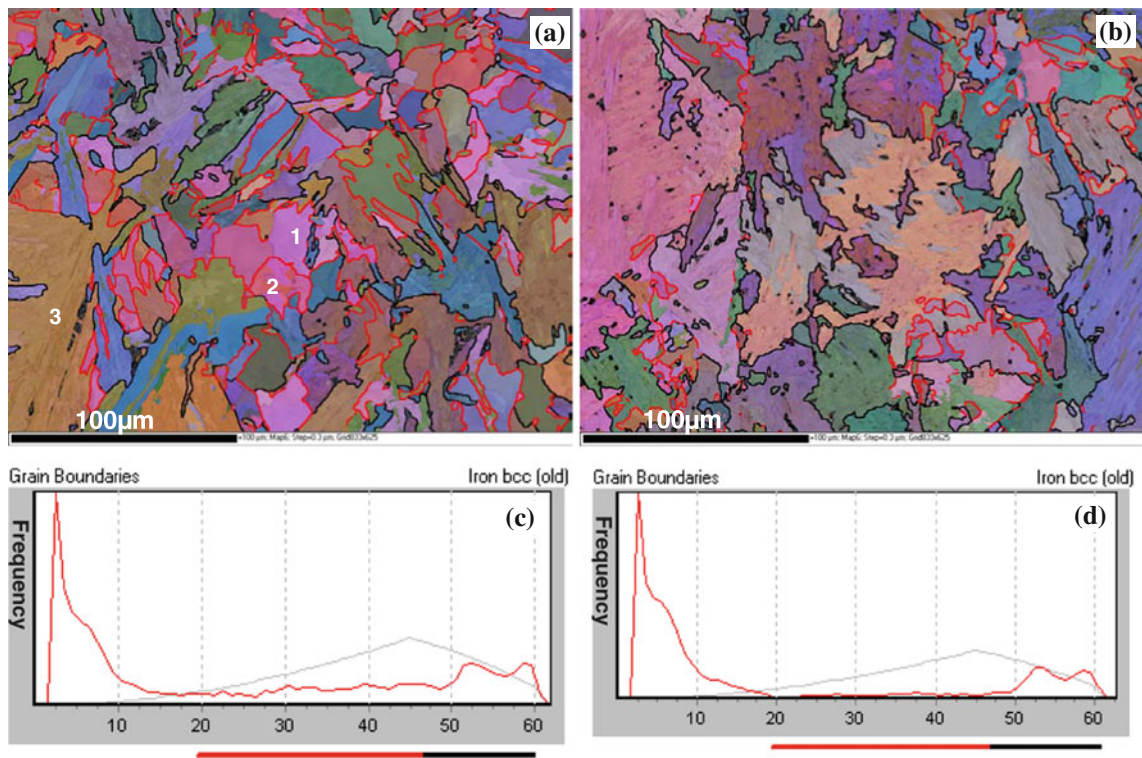
Fig. 3 EBSD orientation map using the all-Euler angles colouring scheme for sample B (**a**) and sample C (**b**), as well as the corresponding grain boundary misorientation distribution profiles of sample B (**c**) and sample C (**d**). The grain boundaries which have a misorientation in the range 20°–48° are highlighted in the images (**a**, **b**) by *red colour*. *1* ferrite, *2* granular bainite, *3* lath bainite (Color figure online)
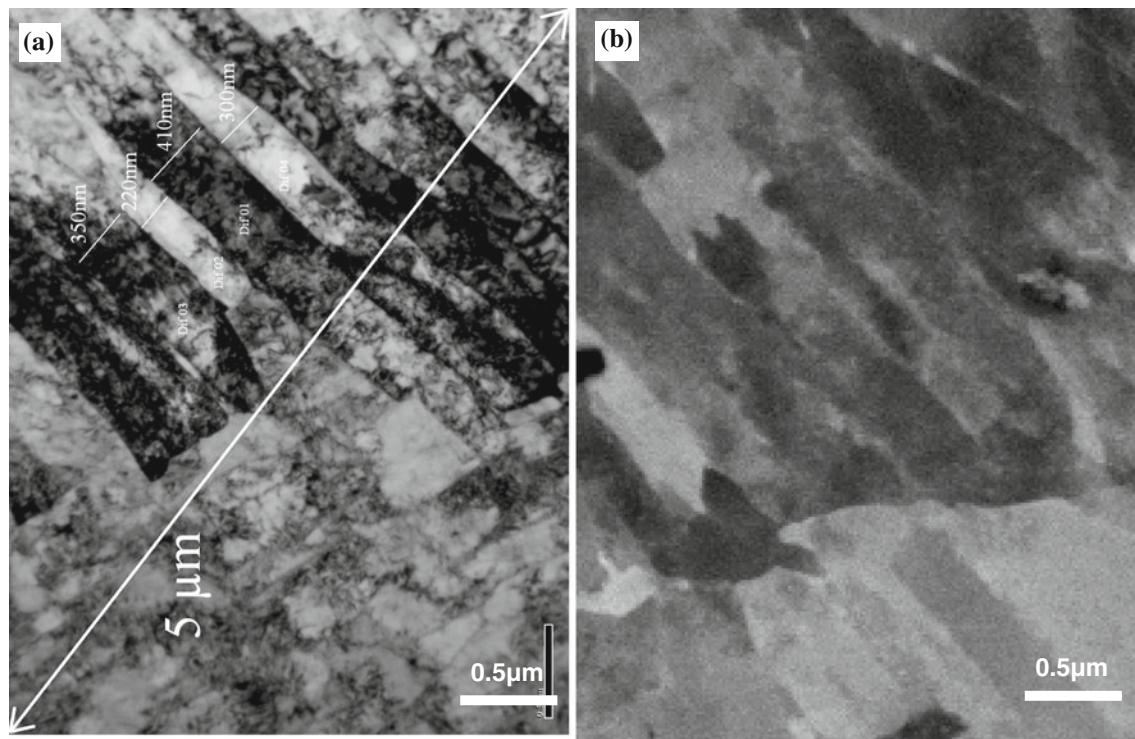

Fig. 4 Lath bainitic structure of sample C observed using **a** TEM and **b** FEG-SEM with BSE mode
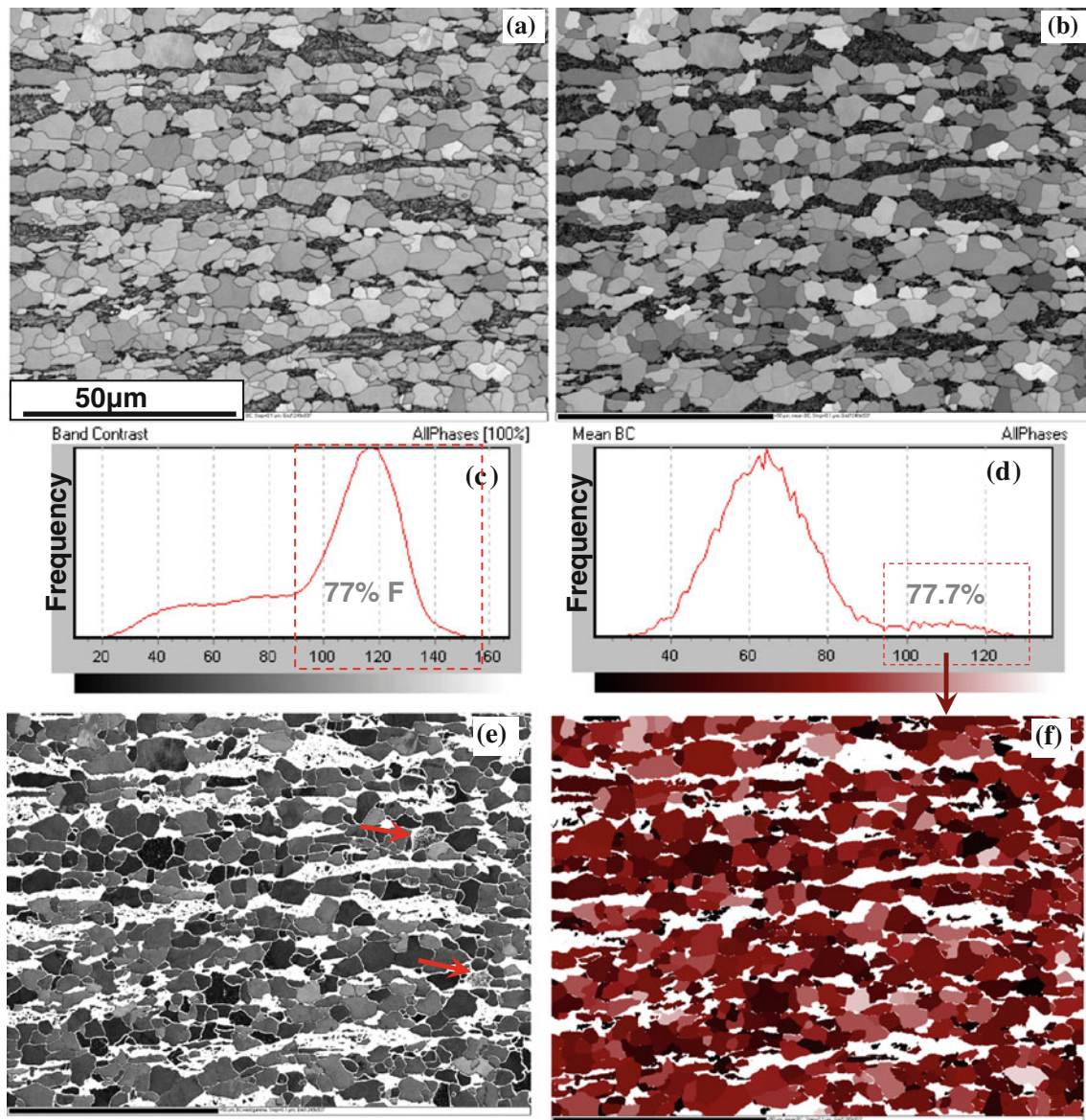
Fig. 5 Advantage of grain unit mode: **a** BC image (pixel mode) and its corresponding BC profile (**c**); **b** mean grain BC image (grain unit mode) and its corresponding mean BC profile **d** of sample F; **e** ferrite separated from martensite using mean grain BC criteria shown in **d**. *Red arrows* in **e** show ferritic grains inside which some pixels are labelled as matersite (Color figure online)

average intensity of the Kikuchi bands with respect to the overall intensity within the pattern, and BS which describes the maximum intensity gradient at the margins of the Kikuchi bands in the pattern should be interesting parameters to distinguish phases. BC and BS can be treated in two ways, i.e. grid/pixel mode and grain unit mode. The BC (pixel mode) and the mean grain BC (grain unit mode) images and their corresponding profiles of sample F have been compared in Fig. 5a, d. It is found that, when BC in pixel mode is used to dissociate ferrite from martensite (Fig. 5c, e), some pixels which should be martensite are labelled as ferrite whereas some other pixels which are inside ferrite grains are labelled as martensite phase (indicated by red arrows). When the mean grain BC is

applied to dissociate these two phases (Fig. 5d, f), a better separation of ferrite from martensite can be noticed in Fig. 5f.

The KAM is calculated by determining the average of all misorientation angles between all neighbour pixels of a given pixel; therefore, it can be used to describe local misorientation gradients in the pixel mode. By contrast, the GIMM or orientation spread (OS) which is defined as the deviation from the average orientation within a grain could be a possible parameter to differentiate phases.

Then, the grain mode treatment of EBSD data is decided to be applied for our study since it makes more metallurgical sense and gives better separation results. In addition, other parameters related to grain unit mode, like grain size
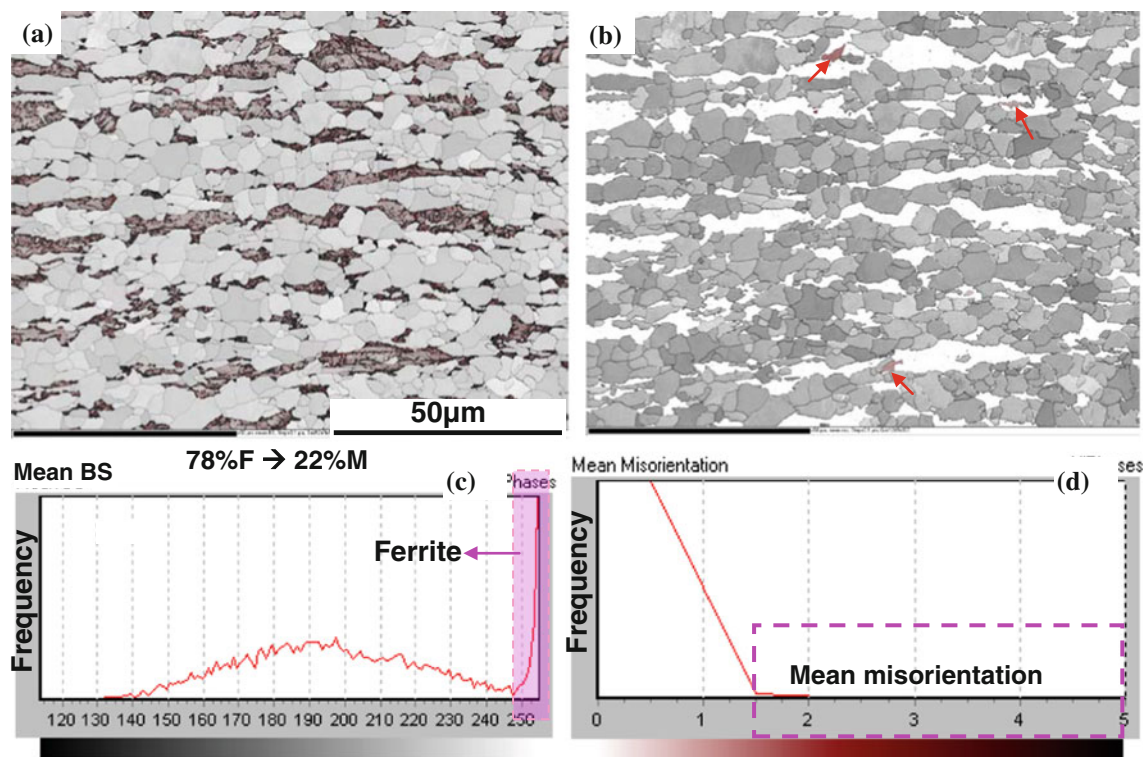
Fig. 6 a Mean BS image and its corresponding mean BS profile c for sample F; b image of the extracted ferrite using mean BS criteria, i.e. the higher mean BS peak in c; d GIMM profile of the extracted ferrite in b. The red arrows in (b) show the few grains that have a mean misorientation higher than 1.5° (Color figure online)

and grain shape, can also be introduced to refine the quantification of phases, since ferrite differs from lath bainite/tempered martensite in grain shape and sometimes in grain size.

Description of the procedure to separate phases

As the grain unit mode will be used in our work, the first step of the procedure is to define grains after noise reduction. It is recognized that, during the successive physical phase transformation of different phases, the former formed phase may influence the crystallography of the later formed phase and therefore create grain boundaries with very small misorientation between them [31, 32].

If the grain boundary misorientation θ that we use to define a grain is larger than this misorientation, then for instance martensite or bainite grains will merge into the adjacent ferrite grains, which leads to an underestimation of martensite or bainite fraction. As the angular resolution of FEG-EBSD is around 1°, a misorientation of 2° is applied for grain boundary definition in our study.

After grain identification, different grain functions like mean grain BC, mean BS, GIMM, grain size and grain shape (aspect ratio) have been used as criteria to separate phases according to the composition (ferrite/bainite/

martensite) and morphology (granular or lamellar) of the microstructure.

The mean BS image and the corresponding mean BS profile for sample F are shown in Fig. 6a, c. It can be seen that the mean BS image gives a very good colour contrast between ferrite and martensite and the mean BS profile presents two distinct peaks. The threshold value at the valley point between these two peaks is chosen to separate the two phases and the extracted ferrite phase is shown in Fig. 6b. The obtained 22 % martensite is consistent with that obtained using conventional metallographic method. Even though, a similar result can be obtained when a threshold value of mean BC profile is used (Fig. 5d, e), it is found that the mean grain BS is a more objective criterion than mean grain BC since its profile peaks that correspond to the two phases are more distinct.

Since GIMM may reflect the substructure inside a grain, it is worth evaluating it in ferrite or bainite phase. A fully ferrite IF steel which contains 0.04 wt% C has been analysed using EBSD and it is found that most of the GIMM in this material is below 1° and the maximum GIMM is around 1.5°. It is known that the ferrite in DP steels close to the martensitic grains has a more significant variation in lattice orientation due to the accommodation of plastic deformation related to martensite transformation [33, 34].

So, the GIMM of the extracted ferrite in sample F (Fig. 6b) has been measured and the frequency profile of GIMM is shown in Fig. 6d. It can be seen that almost all the GIMM of the grains is below 1.5° and the few grains that have a GIMM higher than 1.5° have a bainite morphology. Thus, a criterion of mean misorientation less than 1.5° is to be used to dissociate ferrite from bainite. It should be noted that in the literature, grain OS of recrystallized grains was evaluated to be less than around 1.5° and this value has been used to dissociate the recrystallized fraction from recovered and deformed fractions [35]. When we compare ferrite with recrystallized grains, we find similarities in their microstructure: both ferrite and recrystallized grains have very low density of dislocations and without subgrain structure.

Application of the new phase quantification method

In order to validate the method used to dissociate ferrite and bainite, samples D and E have been analysed using EBSD. As indicated in Table 2, sample D exhibits a complex microstructure composed of a mixture of ferrite, bainite and martensite. This microstructure has been characterised previously using FEG-SEM to obtain a reference value of phase fractions: the ferrite and martensite fractions were determined to be around 31 and 27 %, respectively, by manually point counting on FEG-SEM images (both BSE and SE modes). Figure 7 gives an illustration of the procedure to dissociate ferrite, bainite and martensite using EBSD data in sample D. At first, the martensite is dissociated from bainite and ferrite using mean grain BS criterion. Then, a subset for bainite and ferrite is created (Fig. 7b) and the ferrite can be extracted from the subset using a criterion of GIMM <1.5° (Fig. 7c) leading to a value of 35 % ferrite which is rather close to the reference value of 31 %. Further, it is noticed that a very small quantity of fine laths is still present in Fig. 7c, which is considered to be residual bainite. So, a third criterion, i.e. aspect ratio >2.5, is used to clear out this bainite. In addition, very small grains with a size <0.5 μm^2 have been removed since most of them locate in tempered martensite or on grain boundaries. Finally, a value of 31 % ferrite is obtained (Fig. 7d), which is very consistent with the reference value. It should be mentioned that the volume fraction of martensite obtained using EBSD method (19.5 %) is lower than the reference value (27 %) and this
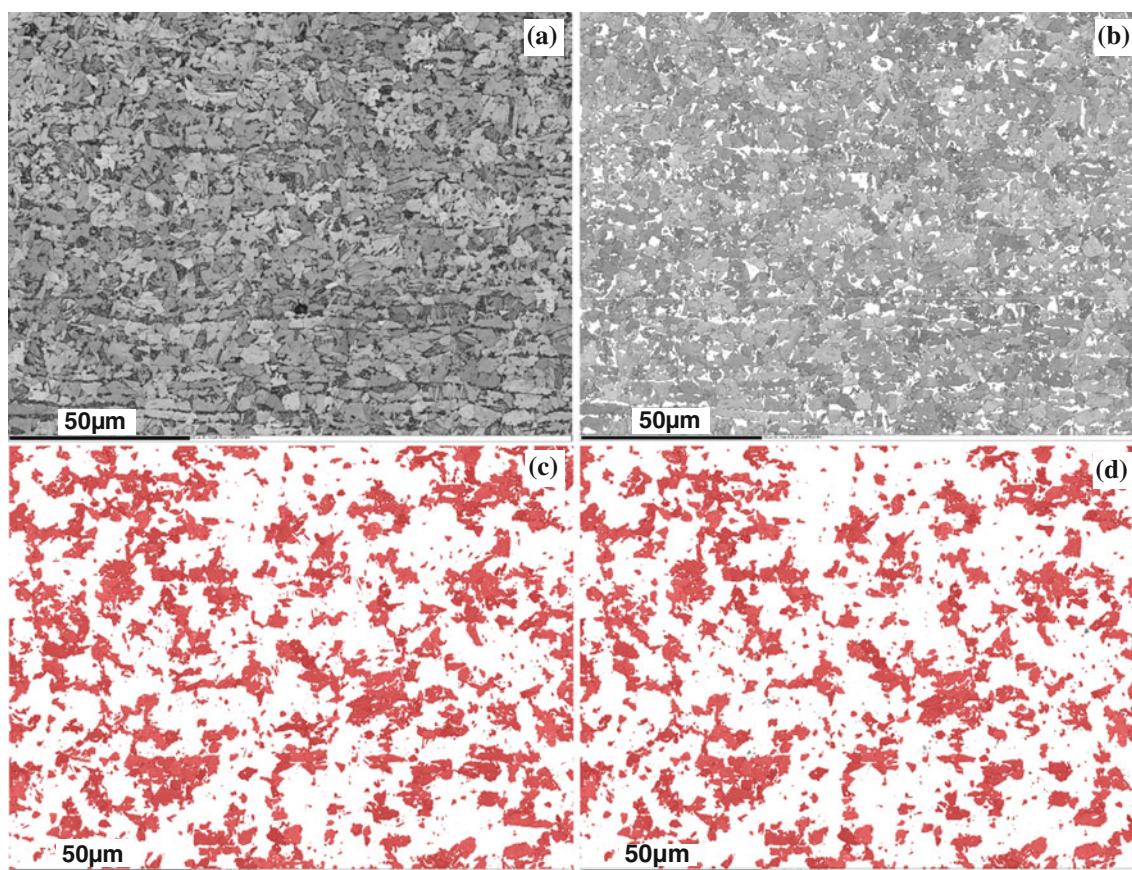

Fig. 7 **a** BC map of sample D; **b** image of the extracted microstructure after removing fresh martensite (19.5 %) using criterion of mean BS (>245); **c** image of the extracted ferrite (35 %) using criterion of GIMM (<1.5°); **d** ferrite in **c** is cleaned up using criteria of grain size >0.5 μm^2 and aspect ratio (<2.5) to remove further the residual bainite and the obtained final ferrite fraction is 31 %
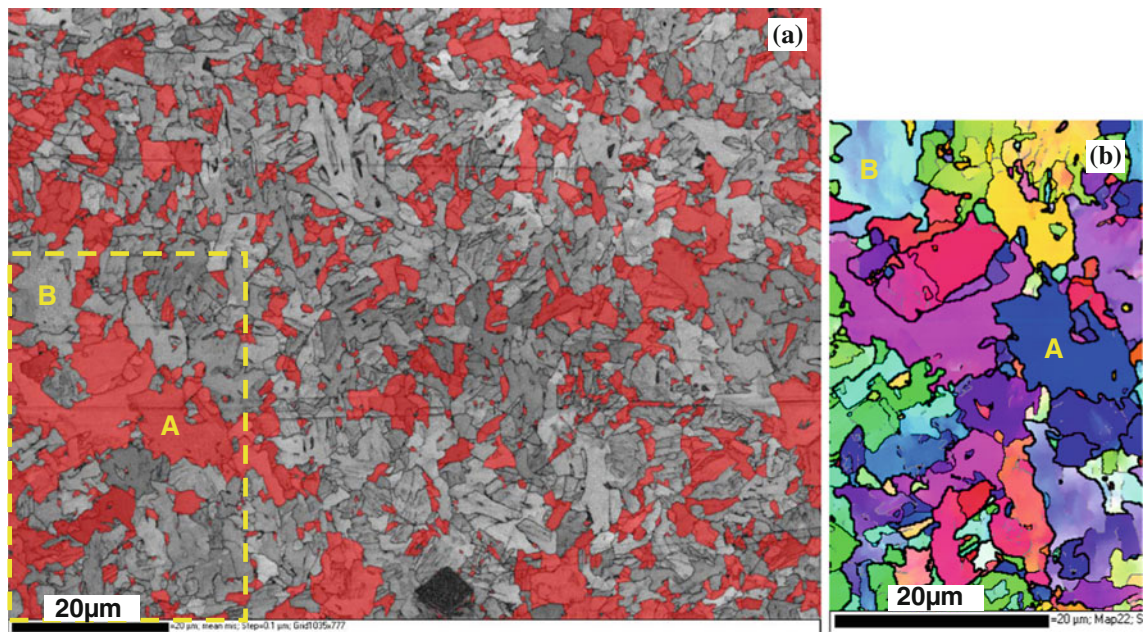
Fig. 8 a EBSD BC image of sample E. The ferrite grains (with GIMM < 1.5°) are highlighted in *red*. **b** Inverse pole figure (IPF) image of the zone indicated by *dashed line* in **a** (Color figure online)

is mainly due to the existence of tempered martensite. Indeed, when the martensite regions with less carbon content is tempered during cooling, the quality of Kikuchi pattern improves significantly, which renders the separation of martensite from ferrite and bainite more difficult. So, the present EBSD method may be reliable to quantify ferrite, bainite and/or fresh martensite but difficult to dissociate bainite from tempered martensite with low carbon content.

The microstructure of the sample E consists of ferrite and bainite. In order to obtain the reference value of the ferrite fraction, the microstructure is quantified not only using coloured etching (metabisulfite) and image analysis, but also dilatometry curve analysis and Thermocalc calculation: the ferrite fraction is estimated to be around 30 %. Using EBSD data, the ferrite is at first separated from bainite using the mean misorientation threshold of 1.5° and a fraction of 33 % is found (Fig. 8a). Then, the few residual bainite laths are removed using the aspect ratio criterion (>2.5) and a value of 31 % ferrite is obtained. Finally, the very small grains with sizes less than 0.5 μm^2 are cleared out from the image to obtain a ferrite fraction of 29.3 %. It is noticed that some grains have the same morphology but belong to different phases, as shown by grains A and B in Fig. 8a. From the EBSD IPF (inverse pole figure) image which is very sensitive to grain internal misorientation, in fact it is found that ferrite grain A has a uniform colour indicating no misorientation inside whereas granular bainite grain B has an orientation variation inside

the grain (Fig. 8b). This shows that the EBSD method can distinguish well the ferrite from granular bainite.

Conclusions

A series of samples displaying various microstructures (ferrite, bainite in the granular or lath form and martensite) have been selected in this study. They have been characterised using different techniques including OM, FEG-SEM (SE and BSE modes), EBSD and TEM. It appears that ferrite cannot be distinguished from granular bainite unambiguously using only OM and/or SEM with SE mode but it was found that FEG-SEM with BSE mode and EBSD are the most suitable techniques to differentiate them. In addition, although the resolution of TEM is much better than that of FEG-SEM (BSE), it is shown that FEG-SEM (BSE) is sensitive enough to reveal very weakly misoriented substructures and this technique can even be used to replace TEM to measure the lath size of bainite.

An automatic phase quantification method using EBSD data has been proposed on the basis of the preceding results. The EBSD data analysis of this method uses the grain unit mode which makes more sense from a metallurgical point of view than the pixel mode and gives the opportunity to analyse further the grain size and morphology and the crystallographic texture of each phase. Clear and new quantitative criteria have been established to separate phases in complex microstructures. For example,

mean grain BS (or mean grain BC) can be used to dissociate martensite from bainite and ferrite; a new criterion like GIMM (<1.5°) can be applied to extract the ferrite from the bainite; other criteria like grain size and shape can be used to provide a more precise phase quantification. This method has been proven to be pertinent and has been validated using several reference specimens.

References

1. LePera FS (1980) J Met 32:38
2. LePera FS (1979) Metallography 12:263
3. Angeli J, Fuereder E, Panholzer M (2006) Pract Metall 43:489
4. Wilson AW, Madison JD, Spanos G (2001) Scripta Mater 45:1335
5. Wu J, Wray PJ, Garcia CI, Hua M, DeArdo AJ (2005) ISIJ Int 45:254
6. Kang JY, Kim DH, Baik SI, Ahn TH, Kim YW, Han HN, Oh KH, Lee HC, Han SH (2011) ISIJ Int 51:130
7. De Meyer M, Kestens L, De Cooman BC (2001) Mater Sci Technol 17:1353
8. Hutchinson B, Ryde L, Lindh E, Tagashira K (1998) Mater Sci Eng A 257:9
9. Petrov R, Kestens L, Wasilkowska A, Houbaert Y (2007) Mater Sci Eng A 447:285
10. Ryde L (2006) Mater Sci Technol 22:1297
11. Zaefferer S, Romano P, Friedel F (2008) J Microsc 230:499
12. Habraken L (1958) In: Proceedings of the fourth international conference on electron microscopy. Springer, Berlin, p 621
13. Qiao ZX, Liu YC, Yu LM, Gao ZM (2009) J Alloys Compd 475:560
14. Wu K, Li Z, Guo AM, He X, Zhang L, Fang A, Cheng L (2006) ISIJ Int 46:161
15. Araki T et al (eds) (1992) Atlas for bainitic microstructures, continuous-cooled Zw microstructures of low-carbon steels, vol 1. Iron and Steel Institute of Japan, Tokyo, p 4
16. Cizek P, Wynne BP, Davies CHJ, Muddle BC, Hodgson PD (2002) Metall Trans 33A:1331
17. Zajac S, Komenda J, Morris P, Dierickx P, Matera S, Penalba Diaz F (2004) Contract No 7210-PR/247, EUR 21245 EN
18. Ohtani H, Okaguchi S, Fujishiro Y, Ohmori Y (1990) Metall Trans 21A:877
19. Ohmori Y (2001) ISIJ Int 41:554
20. Azuma M, Fujita N, Takahashi M, Senuma T, Quidort D, Lung T (2005) ISIJ Int 45:221
21. Krauss G, Thompson SW (1995) ISIJ Int 35:937
22. Wynne BP, Cizek P, Davies CHJ, Muddle BC, Hodgson PD (1997) In: Chandra T, Sakai T (eds) Proceedings of the international conference THERMEC'97, vol 1. TMS, Warrendale, p 837
23. Krauss G, Thompson SW (1994) Final report of Bainite Research Committee. ISIJ, Tokyo 97
24. Steven W, Haynes AG (1956) J Iron Steel Inst 183:349
25. Woo CJ (2003) Metall Trans 34A:2025
26. Zhang Y, Zhang H, Li L, Liu W (2009) J Iron Steel Res Int 16:73
27. Kong J, Xie C (2006) Mater Des 27:1169
28. Du LX, Yi HL, Ding H, Liu XH, Wang GD (2006) J Iron Steel Res Int 13:37
29. Sung HK, Shin SY, Hwang B, Lee CG, Kim NJ, Lee S (2011) Mater Sci Eng A 530:530
30. Huang F, Liu J, Deng ZJ, Cheng JH, Lu ZH, Li XG (2010) Mater Sci Eng A 527:6997
31. Kawata H, Hayashi K, Sugiura N, Yoshinaga N, Takahashi M (2010) Mater Sci Forum 638–642:3307
32. Zaefferer S, Ohlert J, Bleck W (2004) Acta Mater 52:2765
33. Dillien S, Seefeldt M, Allain S, Bouaziz O, Houtte PV (2010) Mater Sci Eng A 527:947
34. Speich GR (1981) In: Kot RA, Bramfitt BL (eds) Fundamentals of dual-phase steels. Metallurgical Society of AIME, Chicago, p 3
35. Mitsche S, Pölt P, Sommitsch C, Walter M (2003) In: Robert L (ed) Microscopy and microanalysis, vol 9. Cambridge University Press, Texas, p 344